JKAU: Eng. Sci., **vol. 16 no. 2**, pp: 17-34 (2006 A.D./1427 A.H.)

A Boundary Element Procedure for the Solution of the Elastohydrodynamic Lubrication Problem of Rolling Line Contacts by a Newtonian Fluid

S. E. SADIQUE*

Department of Mechanical Engineering, National University of Singapore, 10 Kent Ridge Crescent, Singapore –119260.

E-mail: sarder.s@curtin.edu.my

ABSTRACT. The contact characteristics of stiff cylinders lubricated by Newtonian liquids are investigated using hard elastohydrodynamic lubrication (EHL) theory. Numerical modeling is formulated for the coupled set of generalized pressure and plane strain elasticity equations for a finite plane model and a circular representation of the junction under a pure hard rolling line contact using boundary element method. Also a numerical routine is developed to compute film thickness and pressure profiles, and the results are evaluated for a range of possible dimensionless parameters such as speed and load. The hydrodynamic equation is also transformed into a form of boundary integral equation, which is solved by Simpson's rule. The elasticity equation with boundary conditions was solved by constant and quadratic elements based on an iterative procedure by assuming an initial film thickness. The computed results are shown to be amenable to standard boundary element formulation of the EHL problem in the contact region, and show that speed and load have influential effects on the lubricating film shape.

Key Words: Numerical modeling, Boundary element method, Elasto-hydrodynamic lubrication, Hard rolling, Contact behavior.

* Present Address: Lecturer, Mechanical Engineering, School of Engineering and Science, Curtin University of Technology, Sarawak Campus Malaysia, CDT 250, 98009 Miri, Sarawak, Malaysia. Tel: 60 85 44 3939(Office), 60 85 44 3966(Direct).

1. Introduction

A thin lubricant film separates the contact surfaces of the tribo-components where the elastic deformation of the lubricated surfaces cannot be neglected in elastohydrodynamic lubrication. The stiff rollers pressed against each other is frequently encountered in the rolling/sliding machine elements and are often subjected to extremely heavy loads, high speed, and high sliding conditions. The increase of load carried by the concentrated lubricated contacts requires the constant improvement of calculation methods. One of the earliest solutions to the equivalent problem of the lubrication of a cylinder near a plane was presented by Martin [1] considering stiff solids and an incompressible, isoviscous lubricant.

For practical design purposes there have been many attempts to develop appropriate minimum film thickness formulas in tribology. Several numerical solutions of the isothermal elastohydrodynamic problem for cylindrical (line) contacts have been studied by many researchers in the last four decades [2, 3]. Of them, Dowson and Higginson [4] obtained the numerical solution of the isothermal elastohydrodynamic lubrication of line contact by so1ving simultaneously the Reyno1ds and the elasticity equations using inverse method. Since then many methods have been developed. Among them the boundary element method (BEM) became a prominent numerical tool nowadays. The Newton-Raphson method has recently become very popular. Houpert and Hamrock [5] have successfully improved it. They developed an algorithm, which gives the convergent solutions even under extremely heavy loads (to 4.8 GPa) with short CPU times. Karami and Kuhn [6] presented a combined finite element evaluation of hydrodynamic pressure and boundary element calculation of film thickness.

The employment of boundary element would facilitate the calculation of elastic deformation and hence the evaluation of oil film thickness in a more accurate and practical manner for the contacting bodies of complicated shapes under different geometrical and loading boundary conditions. To avoid the complication in computing, an equivalent finite plane model and the circular layer model were introduced in their work. A method which assumes a simple relationship between the pressure and displacement, has been reported in a number of studies, see for example Reference [7]. BEM is simple and the accurate determination of elastic deformation by this method is now well established [8, 9]. Also its extension of applicability to contact problems was also investigated. The integral equations applied in some works represent the

real nature of [10] the contact. The equations are based on a two-dimensional, straight, infinite layer, and solved by either analytical or numerical approximation. In this paper, an attempt is made to formulate the two-dimensional hard elastohydrodynamic lubrication (EHL) problem directly through the boundary element method.

2. Governing Hydrodynamic Theory

Consider the system of two bodies A and B and the fluid layer between them as the basic model of contacting and rubbing solids. The roller contact for the present study is formed by the conjunction of two stiff rollers, which for the dry condition, is typified in Fig.1.

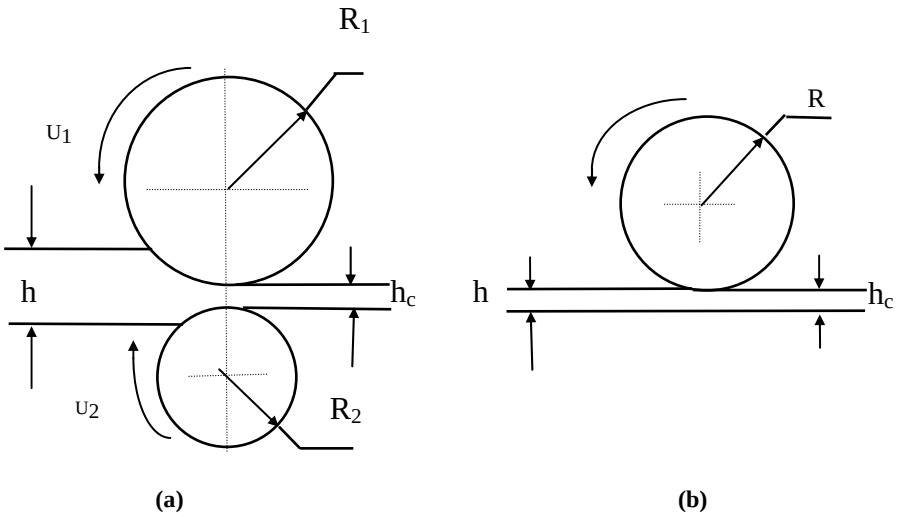

FIG. 1. Line contact geometry: (a) two disks; (b) equivalent contact.

The contact characteristics are to a great extent defined by the roller diameter, speed and load of the rollers. Using the following relationships it is possible to express the governing equations in dimensionless forms:

$$X = x/b,\ \overline{\eta} = \eta/\eta_0,\ H = h/R,\ P = p/E',\ U = \eta u/E'R \quad W = w/E'R$$

The generalized Reynolds equation (no side leakage) for a steady state one-dimensional line contact problem in a lubricant considering isothermal operating conditions and Newtonian fluid can be written in dimensionless form as:

$$\frac{d}{dX}\left(\frac{\overline{\rho}H^{3}}{\overline{\eta}}\frac{dP}{dX}\right) = 24\,U\sqrt{\frac{2W}{\pi}}\frac{d}{dX}\left(\overline{\rho}H\right) \qquad (1)$$

3. Boundary Element Formulation of Reynolds Equation

Isothermal operating conditions and Newtonian fluid are considered. If density remains constant then Reynolds' equation can be rewritten for the classical EHL pressure as

$$\frac{d}{dX}\left(H^{*}\frac{dP}{dX}\right) + \psi = 0 \qquad (2)$$

in which $\psi = -24U\overline{\eta}\sqrt{\frac{2W}{\pi}}\frac{dH}{dX}$, $H^{*}=H^{3}$

3.1 Boundary Conditions

The applied boundary conditions to solve for the pressure distribution in the fluid domain are:

$$P(X_i)=P_i=0$$
$$P(X_o)=P_o=0 \qquad (3)$$
$$\frac{dP}{dX}x_o = P_{io} = 0$$

in which the subscripts *i* and *o* indicate the entrance and exit co-ordinates respectively. By replacing the term ψ in the Reynolds equation with a Dirac delta function δ (*X* - ζ), the following solution can be derived an alternative expression for equation (2) which may be viewed as a field pressure at *X* produced by the flow source δ at ζ. The real pressure distribution in the finite

region can be regarded as the result of a continuous flow supply designated by the term ψ in equation (2) under the constraint of boundary conditions (3). Integral relations are obtained for pressure in the whole domain other than the boundaries X_i *and* X_o. The pressure at point ζ, $P(\zeta)$, explicitly, takes the form

$$P(\zeta) = [-H^*(X_i)G(X_i,\zeta), H^*(X_o)G(X_o,\zeta)]\begin{Bmatrix} P_{ni} \\ P_{no} \end{Bmatrix} + \left[H^*(X_i)\frac{dG(X,\zeta)}{dX}\Big|_{x=x_i}, -H^*(X_o)\frac{dG(X,\zeta)}{dX}\Big|_{x=x_o} \right]\begin{Bmatrix} P_i \\ P_o \end{Bmatrix} + \int_{X_i}^{x_o} \psi(X)G(X,\zeta)dX \quad (4)$$

in which the pressure gradients P_{ni} and P_{no} on the entrance *i* and exit *o* can be found directly from the boundary equations below:

$$P_{ni} = \frac{1}{H^*(X_i)G(X_i,X_o)}\int_{X_i}^{x_o} -\psi(X)G(X,X_o)dX$$
$$P_{no} = \frac{1}{H^*(X_o)G(X_o,X_i)}\int_{X_i}^{x_o} -\psi(X)G(X,X_i)dX \quad (5)$$

3.2 Boundary Element Evaluation of Oil Film Thickness

In boundary element analysis, each body is treated independently and therefore the boundary of each body is discretized as a single domain. Node-pairs are defined on the regions where the hydrodynamic pressure is to be produced (see Fig. 2). The film thickness is therefore calculated at the node-pairs and is equal to the sum of film thickness due to undeformed local geometries of the two bodies at the node-pair, plus the sum of local elastic displacements due to hydrodynamic pressure. If $h_o(PP')$ denotes the undeformed film thickness at node-pair PP' and $d(PP')$ represents the sum of elastic displacements, then

$$h(PP') = h_o(PP') + d(PP') \quad (6)$$

where

$$d(PP') = \delta(P) + \delta(P') \quad (7)$$

where $\delta(P)$, $\delta(P')$ are the displacements in z-directions at node P and P', respectively.

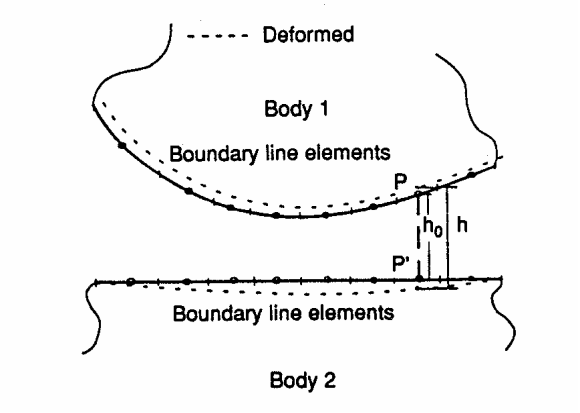

FIG. 2. Contact node-pairs, boundary element and finite element discretization of the contacting surfaces.

3.3 Principle of Virtual Work

For a domain in plain strain condition, the surface displacement u_j and surface traction t_j on the whole boundary are expressed in an integral equation which takes the following dimensionless form [11]:

$$c_{ij}(\xi_0)\bar{u}_j(\xi_0) + \int_{\bar{\Gamma}} \bar{u}_j(\xi)\bar{T}_{ij}(\xi_0,\xi)\,d\bar{\Gamma}(\xi) = \frac{1}{4}\left(\frac{\pi}{8W}\right)^{0.5} \int_{\bar{\Gamma}} \bar{t}_j(\xi)\bar{U}_{ij}(\xi_0,\xi)\,d\bar{\Gamma}(\xi) \qquad (i,j=1,2) \qquad (8)$$

in which c_{ij} is a corner factor, ξ_0 denotes the boundary points under consideration and ξ the points integrated. $\bar{\Gamma}$ is the boundary that is composed of the outer face and the interface between the core and the layer. $\bar{T}_{ij}(\xi_0,\xi)$ and $\bar{U}_{ij}(\xi_0,\xi)$ are the Kelvin solutions that bear the meaning of the traction and

displacement in direction X_i at a point ξ due to a concentrated unit force at point ξ_0 in the direction X_j in an infinite space and they are given in together with expressions for the integrals. Equation (8) leads to the following system of equations after performing the integration:

$$[H]\{U\} = [G]\{T\} \tag{9}$$

Then equation (9) is solved for the displacement of the stiff roller surfaces structure using well-established techniques.

3.4 Film Thickness:

The expression for film thickness can be written as

$$H(X) = H_0 + \frac{X^2}{2R} + \delta(X) \tag{10}$$

where H_0, is the separation of the surfaces at X =0, *R* is the equivalent radius and $\delta(X)$ is the elastic deformation of the contact surfaces to be found from the elasticity equations.

4. Computational Algorithm

The combined physics of the hydrodynamic and the elasticity governing equations are highly non-linear and, hence, in order to arrive at a final solution to the problem, the equations were solved iteratively. The strategic steps applied in the iterative solution procedure were:

1) Appoint an initial value for H_0
2) Find the film thickness from the film thickness equation
3) Solve the Reynolds or generalized pressure equation to obtain a pressure field
4) Determine pressure gradients and then pressure from the equations solved numerically using BEM and
5) Solve elasticity equations to yield deformation from the imposed pressure field, thus updating the film shape.

The pressure and film thickness iterations were continued until both of them converged simultaneously.

5. Analysis of Contacts of Stiff Rollers

To represent the real contact behavior of hard EHL two models are considered in consistency with the present studies and also have a valid agreement with the computed results ($U = 8.15x10^{-11}$, $W = 5.4 \times 10^{-5}$). For the present problem, there are two independent dimensionless quantities. They are W, U for 'hard' EHL problems effect the performance directly. A wide range of possible groups of parameters is selected to study the behavior of the contact. The parameters assumed cover the following ranges: $U = 2.65 \times 10^{-11}$ - 11.65×10^{-11}, $W = 1.4 \times 10^{-5}$ - 7.9×10^{-5}.

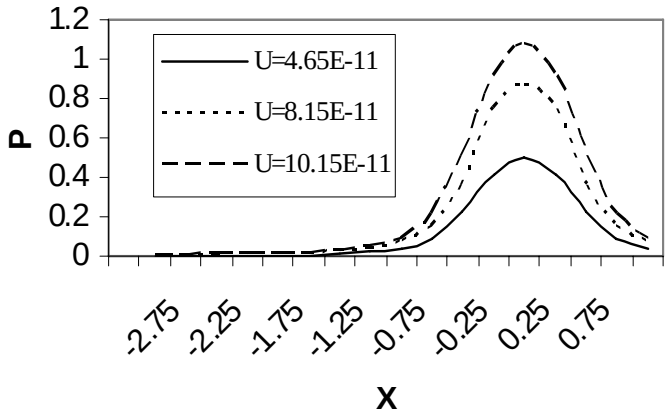

FIG. 3. Effect of parameter U on EHL line contact pressure distribution for an isoviscous flow.

5.1 Effect of Speed Parameter

At low speeds the pressure depends on the contact conditions, while at higher speeds, the film becomes much thicker, the maximum value of pressure increases and the shape of the pressure also changes. In this case, the pressure

depends largely on the natural wedge. Figure 3 illustrates the pressure variation in the contact surfaces of the stiff rollers for nominal rolling speeds corresponding to 4.65×10^{-11}, 8.15×10^{-11} and 10.15×10^{-11} under a stiff contact condition. Those contact pressures that are depicted as progressive in Fig.3 show rather a sharp pressure gradient at the inlet side and less so at the outlet region, which, as a consequence, resulted in a slightly skewed pressure profile towards the inlet region. The maximum pressure was about 0.9. In most of the EHL, contact surfaces are no longer parallel. When comparing the pressure profiles for different linear surface speeds, the width of the pressure zone, which also gives an indication of the actual contact width, can be seen to be slightly wider at the higher speed. The widening of the contact width at higher speed may be attributable to a decrease in rollers modulus, which has resulted in an increase in the deformation of the contact areas. The increase in the roller stiffness (modulus) with increasing speed was presented by Harris [12].

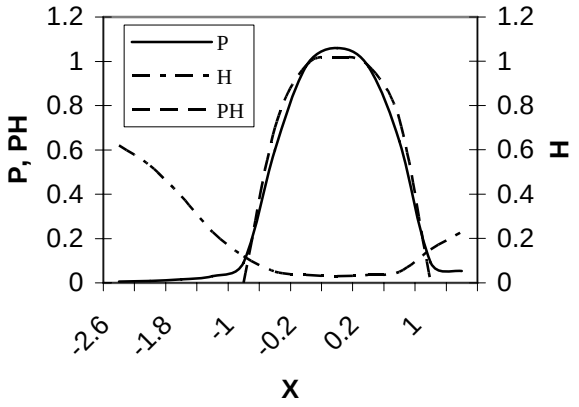

FIG. 4. Effect of speed on pressure, film thickness profiles of EHL.

The general form of the contact pressure distribution is similar to that presented by Karami and Khun [6] and it can be seen to be nearly unaffected by the change in the surface speed. The pressure distributions were found to be symmetrical in shape with no ambient pressures present, which clearly differentiates the nature of the pressures existing in the contact between the roller surfaces. This effectively supports the explanation made earlier about the existence of a non-uniform surface strain in the contact. Nevertheless, the existence of ambient pressure in the present work was in good agreement with the previous work reported [6] in the hard EHL field. The variation of film

thickness (H), the hydrodynamic pressure (P) and Hertzian pressure (P_H) in the dimensionless form, depicted in Fig.4, is included for reference. It is evident that film thickness is largely controlled by the speed parameter under wet conditions. In fact, the profiles are dependent upon the entrance wedge, the formation of film shape and the development of pressure. When comparing the film pressure distributions for different linear roller speeds, it is noticeable that the magnitude of the ambient pressure was smaller at the higher speed. This finding is in good agreement with the results obtained by Dowson [13]. Generally, the trends due to the changes in the speed and the amount of lubricant entrained into the contact were indifferent.

5.2 Effect of Load Parameter

One group of curves reflecting the effect of load parameter W for 2.9 x 10^{-5}, 5.4 x 10^{-5} and 7.4 x 10^{-5} respectively on contact performance is depicted in Fig.5 for a wet contact condition. In this case, the contact width is varied at a value, which represents the pressure characteristics to investigate the effects of different loading conditions. Clearly, the general shape of the pressure distribution changes considerably [14] to that for speed parameter, and the effects of varying the linear load on the pressure distribution and the contact zone are moving slowly over the surface [15]. The peak dimensionless pressure for the load of range was from approximately 0.6 to 1.2, which was only slightly lower than the peak pressure for U. This means that the contact pressure does not increase proportionally with the level of speed parameter. As would be expected, they exhibited a lower pressure excursion, as the thin film separating the two rollers would further deform the surfaces, hence increasing the overall sub-surface stresses. This is consistent with the conclusion that the contact width is widened for a stiff contact when compared with a Hertzian contact.

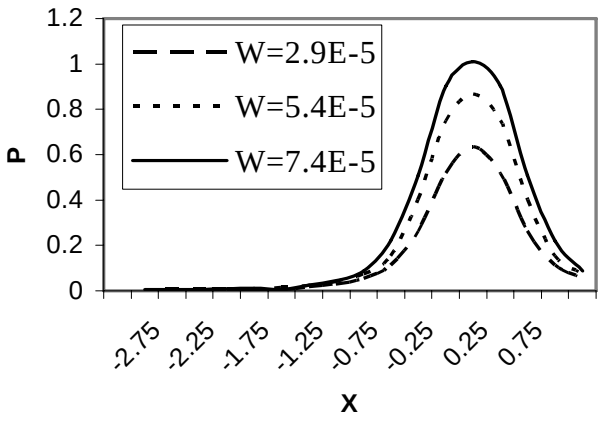

FIG. 5. Influence of various loads on pressure profiles of EHL.

5.3 Film Thickness

5.3.1 *Analysis by Finite Plane Contact Model*

The results from this calculation set are presented in Fig.6**,** dividing the boundary into 24 constant elements. With regard to the film thickness, it can be seen that a large pressure exists within the contact. However, when the film thickness (H) is considered, a smaller value is observed due to the higher loading and reduced speeds. Similar results have been observed and reported by Wolff et al [15].

5.3.2 *Analysis by Circular Contact Model*

To represent the true roller geometry, a circular layer was analyzed with quadratic elements where a radius of R = 0.02 m was used and W = 5.54 x 10^{-5}, U = 8.15 x 10^{-11}, ν = 0.3. The boundary on which the pressure acts was divided into 12 quadratic elements. The results from this analysis are shown in Fig.7, which shows clearly the progressive film thickness buildup in the inlet zone. Under this circumstance, the effect of the solid roller surface becomes more significant and the junction becomes hard in nature. The results for the two methods are closely similar in spite of the large contact width, the effect of the curvature and the difference in the numerical discretization.

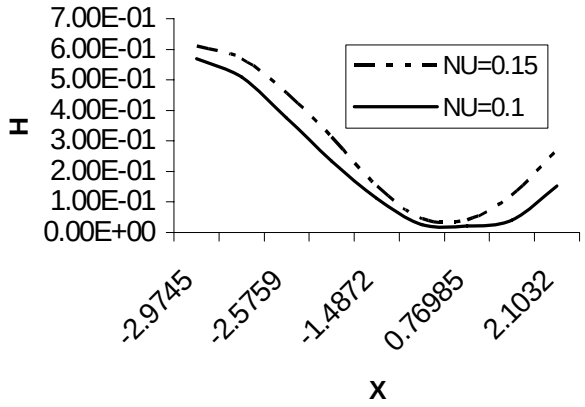

FIG. 6. EHL line contact film thickness for an isoviscous flow where υ (NU) is Poissson's ratio (24 uniform elements).

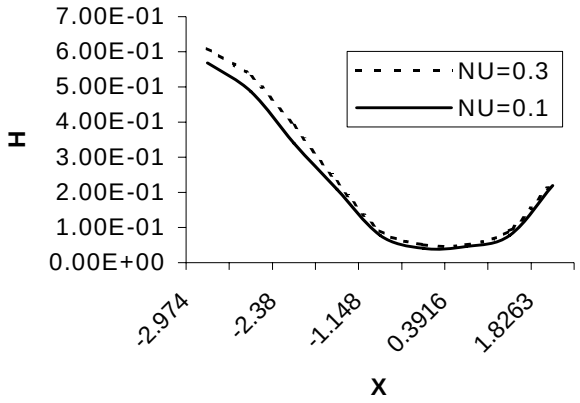

FIG. 7. EHL line contact film thickness for an isoviscous flow where υ (NU) is Poissson's ratio (12 quadratic elements).

6. Comparison of Pressure and Film Thickness with Previous Studies

It can be seen from Fig. 8, Fig. 9 and Fig. 10 that the baseline hydrodynamic model developed shows valid agreement with the published results from [6, 16] which confirms the foundation with regard to this work. Nevertheless, to check the correct functioning of this model, by allowing the flow exponent, the fluid appears to be significant. Therefore, this confirms the

correct functioning of the computer program developed at this time. To confirm the basis of the numerical model developed so far, the computed pressure and film thickness profiles for a Newtonian fluid characteristic are compared with published results from Xue et al (16) and Karami and Kuhn (6) as shown in Figs. 8, 9, and 10 for both cases.

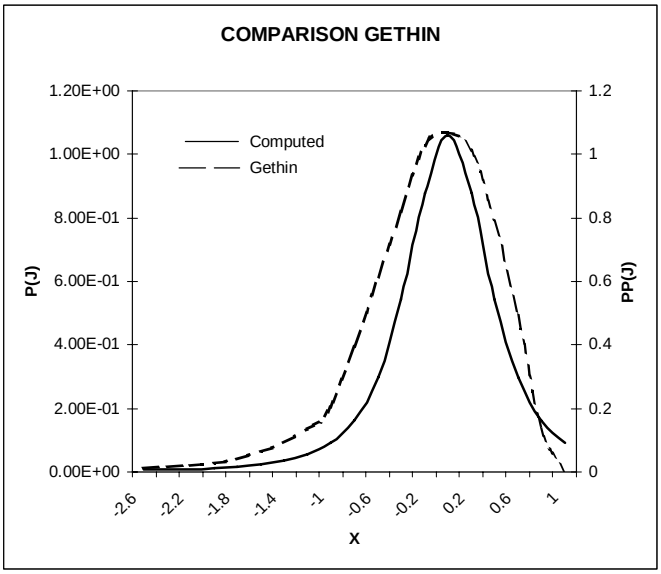

Fig. 8. Stiff - isoviscous hydrodynamic models comparison with published work [Xue et al.'s model (16)].

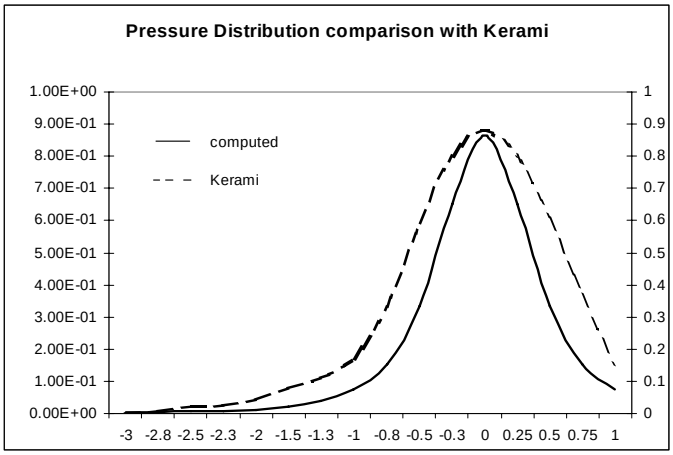

FIG. 9. Stiff - isoviscous hydrodynamic models comparison with published work [Karami and Khun model (6)].

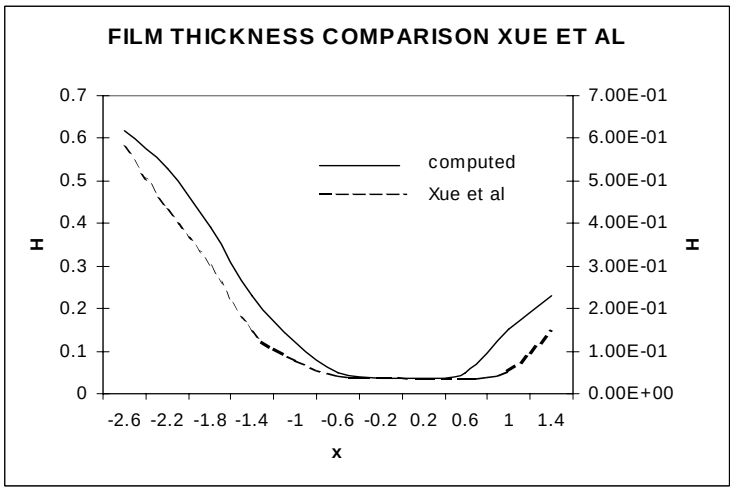

FIG. 10. Film thickness comparison curves with Xue et al's model (16).

The conditions used in the comparative study for these cases are itemized and some of the important results obtained from this study are also listed in Table 1.

TABLE 1. Results from the numerical comparison study.

Parameters	Karami and Kuhn (6)	Present Study	Xue et al (16)	Present Study
Max. Pressure, p_{max}	0.88	0.85	1.067	1.06
Min. film thickness, h_0	0.039	0.0359	0.0342	0.035

7. Conclusions

BEM is a unified treatment of the elastohydrodynamic lubricated contact problems using the boundary element technique at high speeds and high loads. The method can be implemented with low computing times on a computer by solving Reynolds and elasticity equations simultaneously. Based on the computed results, the following advantages are noticed:

1. The new approach is in very good agreement with the complete solutions of boundary integral equations and provides an easy and accurate way to solve such stiff-roller contact problems.
2. Boundary quantities can easily be solved numerically and satisfactory simultaneous convergence is obtained for the applied parameters.
3. The use of equation condensation reduces the computational effort because fewer unknowns are involved. It also seems to be a very interesting alternative and a natural modeling approach in surface mechanics.
4. This method requires a few discretized elements in the contact zone, and avoids solving algebraic equations, which is influential and significant to obtain hydrodynamic pressure.

Acknowledgment

The work reported in this paper was supported by the Institute of Advanced Technology, University Putra Malaysia and Material Science Division, Department of Mechanical Engineering, National University of Singapore, and the author conveys his appreciation for this support.

Notation

C_{ij} = corner factor

$E^{/}$ = equivalent elastic modulus

H = lubricant film thickness

H = dimensionless film thickness

i = entrance

o = exit

P = pressure

P_i = entrance pressure

P_o = exit pressure

P_{ni} = pressure gradient at X_i

P_{no}= pressure gradient at X_o

P_H = Hertzian pressure

P = dimensionless pressure

R = reduced radius

R_1 = radius of upper roller

R_2 = radius of lower roller

t_j = surface traction in x_j direction

u_j = surface displacement in j direction

U = dimensionless speed parameter, $\eta_0 u/E^{/}R$ or mean surface velocity in x direction, $1/2(u_1+u_2)$

υ = Poissson's ratio

η = dynamic viscosity coefficient

$\overline{\eta}$ = dimensionless viscosity, η/η_0

w = load per unit length of ooller

W = dimensionless load parameter, $w_z/E^{/}R$

X = dimensionless coordinate

X_i = entrance coordinates of film

$\overline{\rho}$ = lubricant density

X_o = exit coordinates of film

ξ = boundary point under consideration

ψ = a term in Reynolds equation

η_0 = viscosity at atmospheric pressure

δ = Dirac delta function/ displacement

References

[1] **Martin, H.M.,** Lubrication of Gear Teeth, *Engineering, London,* **102,** 199, (1916).

[2] **Archard G.D., Gair, F.C.** and **Hirst, W.,** The elastohydrodynamic lubrication of rollers, *Proc. Roy. Soc. Series* A, **262**, 5, (1964).

[3] **Dowson, D.** and **Whitaker, A.V.,** The isothermal lubrication of cylinders, *A.S.L.E. A.S.M.E. International Lubrication Conference Washington, D.C., Amer. Soc. lubric. Engrs Preprint* **64-LC22**, (1964).

[4] **Dowson, D.** and **Higginson, G. R.,** Elastohydro-dynamic Lubrication, Pergamon, Oxford, (1977).

[5] **Houpert, L. G.** and **Hamrock, B. J.,** A Fast Approach for Calculating Film Thickness and Pressures in Elastohydrodynamically Lubricated Contacts at high Loads, *ASME- Journal of tribo1ogy*, **108,** pp. 411- 420, (1986).

[6] **Karami, G.** and **Kuhn, G.,** A finite element-boundary element treatment for the analysis of elastohydrodynamic lubrication problems, *Computational Mechanics,* **14, pp.** 289-297, (1994).

[7] **Higginson, G. R.** The theoretical effects of elastic deformation of the bearing liner of journal bearing performance, *Proc. Instn. Mech. Engrs.,* **180,** pp.31-38, (1965-1966).

[8] **Brebbia, C.A., Telles, J.C.F.** and **Wrobel, L.C.,** Boundary element methods techniques. *Springer-Verlag,* Berlin, 1984.

[9] **Cruse, T.A.,** Recent advances in boundary element analysis method. *Comp. Meth. Appi. Mech. Engng.,* **62,** pp. 227-244, (1987).

[10] **Karami, G.,** Boundary element analysis of two-dimensional elastoplastic contact problems. *Int. J. Num. Meth. Engng.,* **36,** pp. 221-235, (1993).

[11] **Banerjee, P.K.** and **Butterfield, R.,** Boundary element methods in engineering science. *Mc-Graw Hill,* New York, (1981).

[12] **Harris, T.A.,** Roller Bearing Analysis, 3rd edition, *John Wiely and Sons, Inc.*, New York, USA.

[13] **Dowson, D.,** Investigation of cavitation in lubricating films supporting small loads, *Inst. Mech. Engrs., Proc. of the Conference on Lubrication and Wear*, 93-99, (1957).

[14] **Gakwaya, A.,** A boundary element formulation for the thermo-elastohydrodynamic contact problems Part I: theory, *Engineering Analysis with Boundary Elements,* **10,** pp. 1-15, (1992).

[15] **Wolff, R., Nonaka, T., Kubo A.** and **Matsuo, K.,** Thermal elastohydrodynamic lubrication of rolling/sliding line contacts, *ASME Journal of Tribology*, **114,** pp. 706- 723, (1992).

[16] **Xue, Y.K., Gethin, D.T.** and **Lim, C.H.,** Elastohydrodynamic lubrication analysis of layered line contact by the boundary element method, *International Journal for Numerical Methods in Engineering*, **39,** pp. 2531-2554, (1996).

استخدام أسلوب العناصر المحيطة في حل مشاكل التزييت الهيدروديناميكية المطاطية بواسطة موائع نيوتن للأجزاء المتدحرجة

ساردر الياس صديق

قسم الهندسة الميكانيكيه بالجامعه الأهليه بسنغافورة

تم فى هذا البحث فحص خصائص الالتصاق لاسطوانات صلدة تـم تزييتها بواسـطة سـوائل نيـوتن واسـتخدام نظريـة التزييـت الهيدروديناميكية المطاطية. كما تم تمثيل النمـوذج العـددي للفئـة المزدوجة للضغط فى الحاله العامه ومعادلات الجهد الانفعالي المرن المستوى المحدد ودائرة الملتقى عند نقطـة الالتـصاق مـع خـط التدحرج، وذلك بطريقة العناصر المحيطة.

وقد تم التوصل إلى طريقة لاستخدام الحساب العددي لحساب شكل التغير في سمك غشاء الزيـت والـضغط واسـتنتاج الحيـز المسموح للكميات غير البعدية التي تعتمد على السرعة والحمل. كما تم تحويل معادلة الهيدروديناميكا إلى معادله تكاملية محدده، وهذه قد تم حلها بواسطة قاعدة سيمبسون. كما تم حل معادلة المرونـة مـع

وقد تم عرض النتائج المحسوبة التي ثبت ضرورة وجودهـا كمقياس لتمثيل العنصر المحدد للمشكلة في حيز الالتـصاق، كمـا وضح تأثير السرعة والحمل على شكل غشاء التزييت.